Optimization of the accelerators for the ITER Neutral Beam Injector project

V. Antoni, P. Agostinetti, M. Cavenago[a], H.P.L. de Esch[b], G. Fubiani[c], N. Pilan, G. Serianni, P. Veltri
and the NBI RFX Team

Consorzio RFX Euratom-ENEA Association, Padova, Italy
[a]INFN-LNL, Legnaro, Italy
[b]Association EURATOM-CEA Cadarache, IRFM/SCCP, France
[c]CNRS, LAPLACE, F-31062 Toulouse, France

M. Kashiwagi, M. Taniguchi, N. Umeda, T. Inoue
Japan Atomic Energy Agency, Japan

A joint Japan-EU R&D activity is in progress to optimize the accelerator for the ITER NBI. The accelerator baseline design is based on a five grids system which can be adapted to operate with three grids for initial operations at low voltage (500 kV). Moreover, in order to speed up the test of the NBI system at the Test Facility, a negative ion source with extraction voltage up to 100 kV will be operated in parallel to the full injector.
In this contribution the three accelerators mentioned above are presented discussing the procedure to optimize the grid geometry in order to assure optimum optics during operation when the grids undergo deformations and thermal stresses due to the particles that hit their surface

1. Introduction

Two Neutral Beam Injectors (NBI) are foreseen in ITER in order to deliver a total of 33 MW of heating power. Each NBI is designed to operate at 1 MV and 40 A current in Deuterium and at 870 kV and 46 A in Hydrogen [1,2]. In recent years a joint revision of the NBI design for ITER performed by the Japan and EU Domestic Agencies in close contact with ITER has led to important changes which have improved the availability and reliability of the NBI system [3]. The insertion of an absolute gate valve between the NBI and the duct and the modification of the Beam Line Vessel with possibility of vertical access, have improved the availability of the system while shortening the time required for maintenance and repair in case of fault. The adoption of the air insulated High Voltage deck and the choice of the RF Ion Source have led to less demanding maintenance for the source which does not require replacements of the filaments as it was for the arc driven source [4]. Passive and active protection systems for the accelerator grids and power supplies are now implemented in the project therefore improving the reliability of the system. Finally the design of the Test Facility to be built in Padova and

aimed to test and optimize the NBI and to assist the operations in ITER has been almost completed [5]. A robust R&D program is in progress at the 1 MV test facilities in Naka (JAEA) and Cadarache (CEA) to tackle and solve the remaining issues related to High Voltage holding and particle acceleration in the 1 MV range [6,7,8]. To assess a multi-aperture multi-grid (MAMuG) and a single-aperture single-gap (SINGAP) accelerator [9] concepts at the same test facility with the same diagnostics, a collaborative R&D was performed between JAEA and CEA Cadarache under an ITER task agreement. As a result of better voltage holding and less electron acceleration, the MAMuG was confirmed as the baseline design for ITER [6,8]. All these activities have led to a better understanding of the physics of the 1 MV accelerator and of the negative ion extraction which have allowed the accelerator design to be further advanced as discussed in the following.

2. The accelerator design

In the ITER NBI baseline design the accelerator is a MAMuG system based on five grids [10]. In order to provide auxiliary heating to the initial operation of ITER in Hydrogen and relatively low current, it has been

proposed to operate one of the NBI as a three grid system at a reduced voltage of 500 kV. It has been verified that the present grid support structure and power supply layout can easily be adapted to a three grids system. In this contribution three accelerators of interest for ITER, namely the five-grids 1 MV accelerator in the reference design, the three-grids 500 kV accelerator foreseen for initial operations and the single grid 100 kV accelerator to optimize the extraction in the Ion Source are presented. The criteria and the method applied to optimize the accelerator design are described. In particular the design of the accelerator grids has to provide optimum perveance, compatible with the finite size of the grids due to the cooling channels and the insertion of permanent magnets required to deflect the unwanted electrons co-extracted from the source or generated by stripping losses. The thermo-mechanical analysis of the grids has been performed by taking into account the power load due to co-extracted and secondary electrons. In order to minimize the grid bending and the thermal stresses the grids are actively cooled and the cooling channels have been carefully designed in order to be accommodated in a relatively narrow space.

The optimization process is therefore based on a sequence of the following steps which are reiterated up to final convergence:

a) The initial electric field distribution is computed.
b) The magnetic field distribution as obtained from the combination of magnetic filter and permanent magnets inserted in the grids is added
c) The particle trajectory is computed.
d) The interaction with the background gas is simulated by evaluating the stripping losses and the generation of secondary particles due to interaction of primary particles with material surfaces.
e) The new electric field distribution due to the charge distribution and the related trajectories are calculated up to convergence.
f) The thermal load due to ions and electrons intercepting the grids is evaluated and the deformation, when the cooling is applied, evaluated. The design of the grids (cooling channels size and layout and position of permanent magnets) is modified in order to minimize the deformation.
g) Steps from a) to f) are repeated until an optimum configuration is obtained for a single or a couple of beamlets.
h) Interaction among beamlets is evaluated to compensate for the divergence of the beamlets by a suitable mechanical displacement of the apertures

These steps are accomplished using different codes. The electric field and the initial trajectories are computed by using the code SLACCAD [11,12] and then by adding the magnetic field distribution. Recently a new code BYPO [13], which solves in a self-consistent way the trajectories with an initial distribution of magnetic and electric field, has been developed and the results applied to benchmark the results of SLACCAD. The interaction of the particles with background gas and material surfaces are described by the Monte Carlo Code EAMCC [14]. The thermal analyses are performed by using ANSYS. Finally the beamlet-beamlet interaction is studied by using the code OPERA [15]. This procedure has been applied to the optimization of the highest priority accelerator, namely the low voltage one, as in the present planning it is expected to enter into operation in three years from approval. This accelerator shares several characteristics with the accelerator required by the diagnostic neutral beam (DNB) [10] for operation in Hydrogen, so that the initial development of the accelerator has been performed in parallel with that of the DNB. The main requirements of this accelerator are a current of 60 A H⁻ (and later 40 A D⁻) and an energy of 100 keV. In Fig. 1 a comparison of the beam profile for the three accelerators is shown.
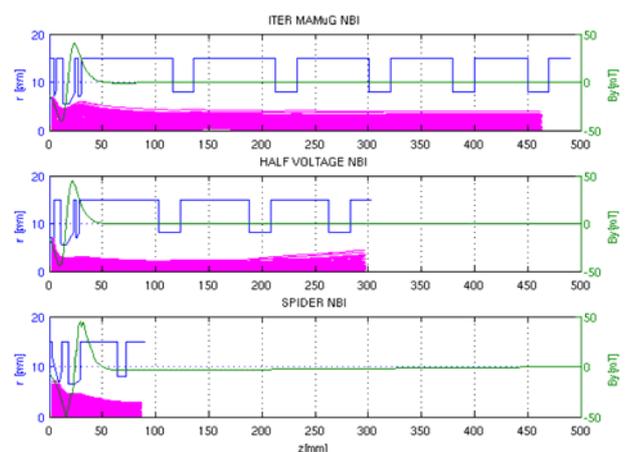

Fig. 1 - Ion beam trajectories simulated with SLACCAD. Also the aperture profiles and the magnetic field by suppression magnets is sketched.

3. Study of the beam optics
All three accelerators work with multi-aperture grids biased at different potentials. Each grid features 1280

apertures. All systems have a Plasma Grid (PG) and an Extraction Grid (EG - at approximately 10 kV). The accelerations steps are respectively:

- 5 acceleration grids for ITER MAMuG (5 acceleration steps of 200 kV each)
- 3 acceleration grids for ITER Half-Voltage (3 acceleration steps of about 160 kV)
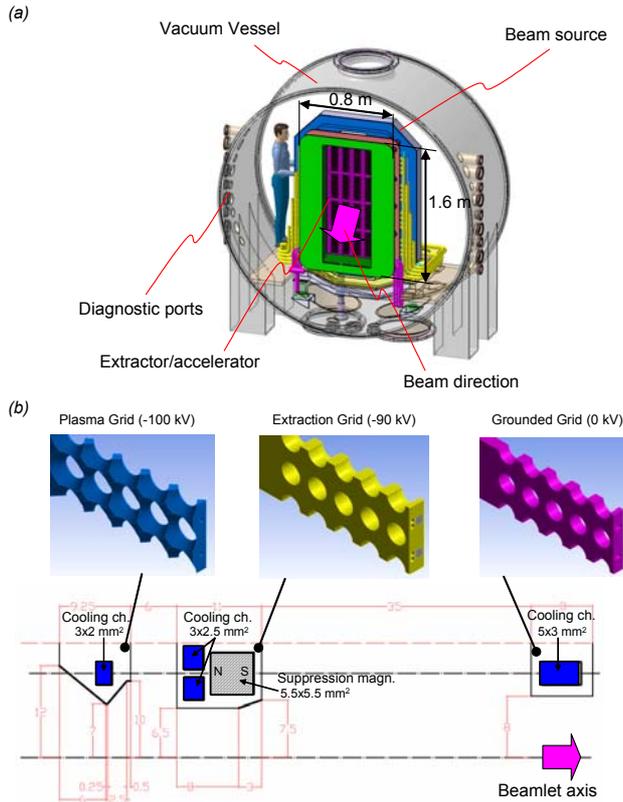- 1 acceleration grid for SPIDER (a single acceleration step of 90 kV)

Fig. 2 - Scheme of the grids for the 100kV accelerator: (a) Design overview; (b) Detailed view of the grids.

In Fig. 2 a scheme of the grids for the low voltage accelerator is shown. The negative ion trajectories, calculated with the SLACCAD code, are shown in Fig. 3. The interactions among particles inside the accelerator, like secondary particle production processes, are studied by the code EAMCC [14]. This is a 3-dimensional (3D) relativistic particle tracking code where macroparticle trajectories, in prescribed electrostatic and magnetostatic fields, are calculated inside the accelerator. In the code, each macroparticle represents an ensemble of rays. This code needs as inputs the electric and magnetic fields inside the accelerator. The former was calculated with SLACCAD, as explained above. The latter was calculated

by summing the field given by the SmCo permanent magnets and the field from the plasma grid filter current (calculated by assuming an infinitely thin electron sheath). Collisions are described using a Monte-Carlo method. The various kinds of collisions considered in the code are: (i) electron and heavy ion/neutral collisions with grids, (ii) negative ion single and double stripping reactions and (iii) ionization of background gas.
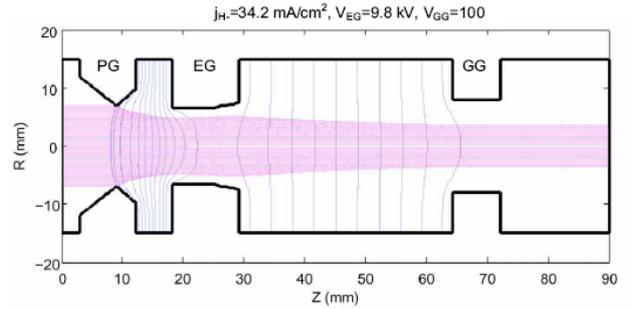

Fig. 3 - SLACCAD simulation of the beam optics: equipotential lines (blue) and particle trajectories (magenta) are estimated by integration of the Poisson's equation.

In Fig. 4 the trajectories of negative ions and of co-extracted and stripping loss electrons for a single beamlet are shown. The corresponding thermal load is also shown [16]. The PG is heated by the plasma inside the RF ion source, with a surface power density that is estimated to be about 20 kW m^{-2} [17]. This grid is required to operate at a temperature of about 150°C in order to enhance the negative ion surface production due to cesium evaporated inside the main chamber. For this reason the grid is also Molybdenum coated on the side facing the plasma. The apertures are designed with conical chamfers on the upstream and downstream sides of the grid. A larger surface for ion production is obtained with this solution, and its efficacy has been demonstrated by experimental results [18]. A 4 kA current flows in the vertical direction, to provide a horizontal magnetic field that reduces electron temperature and the number of co-extracted electrons. The EG has an electric potential that is about 10 kV higher than the PG, so that the negatively charged ions can be properly extracted from the RF expansion chamber. Suppression magnets, embedded in the grid, have the function to deviate the trajectories of the co-extracted electrons, making them collide with the grid surface. The consequent power loads are quite high and concentrated, hence this grid is the most critical from the structural point of view, and is

designed with a high performance cooling system. The grounded grid (GG) has the function to accelerate the ion beamlets up to a potential of about 100 kV, and is also loaded by co-extracted and stripping electrons.

While the EG is heated mostly by the co-extracted electrons, the heat on the GG is approximately half coming from the co-extracted electrons, and half from the secondary electrons due to stripping and surface reactions.

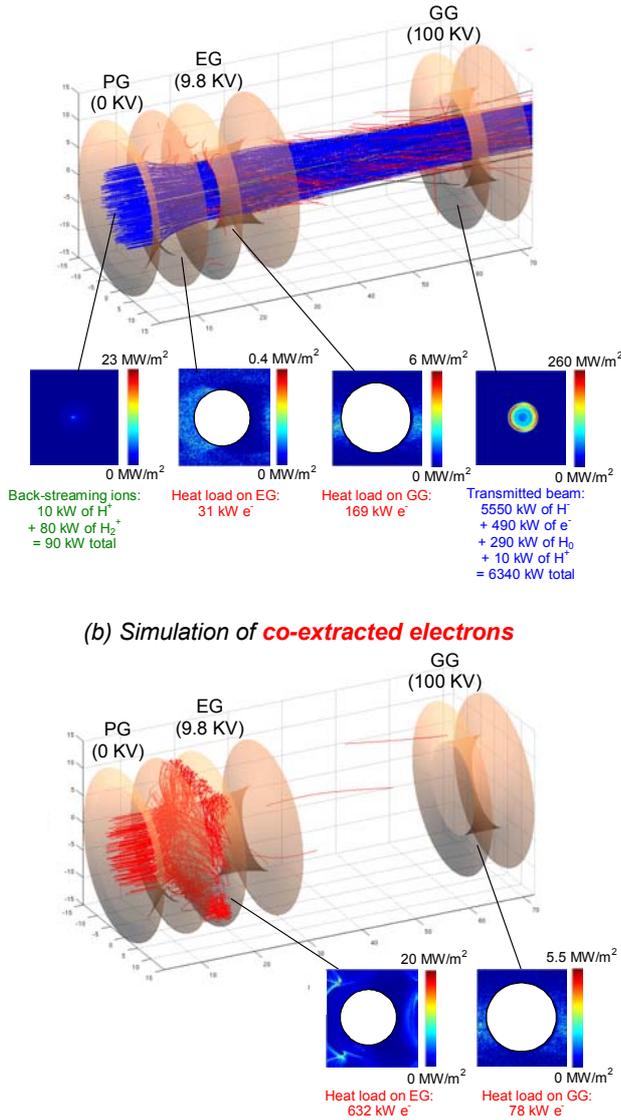*(b) Simulation of co-extracted electrons*

Fig. 4 - EAMCC simulation (a) of a negative ion beamlet and (b) of the co-extracted electrons in the 100 kV accelerator: the particle trajectories and stripping reaction are simulated with a Monte Carlo approach in a domain with electrical and magnetic fields. The power corresponding to the whole accelerator (1280 beamlets) is reported.

The transmitted beamlet power distribution features a ring that is hotter than the central part. These could be due to the chamfered shape of the PG apertures. In fact, this effect is reversed in case of a flat PG surface [16].

The backstreaming positive ions are concentrated in the center of the aperture area. The consequent heat power density is quite high, as it covers only an area of some tens of square millimeters. These ions could give rise to sputtering phenomena on the plasma source back plate and on the driver Faraday shields, with a consequent decay of the plasma purity and problems of surface integrity. The sputtering yield due to the backstreaming deuterium ions is generally reduced by a factor of about 5 if the copper surface is coated with Molybdenum. Hence, in order to minimize the detrimental effects consequent to sputtering, a layer of Molybdenum of some microns is foreseen to be applied on the plasma source back plate.

4. Thermo-mechanical optimization

The accelerator grids must be designed in such a way that the corresponding apertures are well aligned during all the operating scenarios, in order to obtain good beam optics. For this reason and for manufacturing requirements they are vertically split in four segments, independently supported with a fixed pin at the left side and with a sliding pin at the right side [16]. For optical reasons, the maximum allowable misalignment between the corresponding apertures of the three grids is fixed to 0.4 mm, whose 0.2 mm due to thermal expansion.

The grids have also to withstand two categories of stresses:

a) Cyclic thermal stress due to the temperature gradients between hotter and colder zones. These stresses must be maintained low in order to satisfy the requirement on fatigue life.

b) Static stress due to the water pressure. The local values of equivalent stress must be lower than the allowable values for electrodeposited copper (fixed at 100 MPa). The position and dimensions of the cooling channels, as well as the water flow, must be optimized in order to satisfy all the requirements on alignment and stresses according to the ITER criteria [19] and in all scenarios (conditioning, partial power, full power etc.).

Several analyses have been performed to estimate the temperatures and stresses along the grids [20]. Fig. 5 shows the results for the reference operating conditions at 100 kV. It appears that the thermal stresses are causing

also an out-of-plane deformation of the grids. The analyses have shown that these deformations can be minimized in order to keep within tolerable values the increase in the beam divergence.
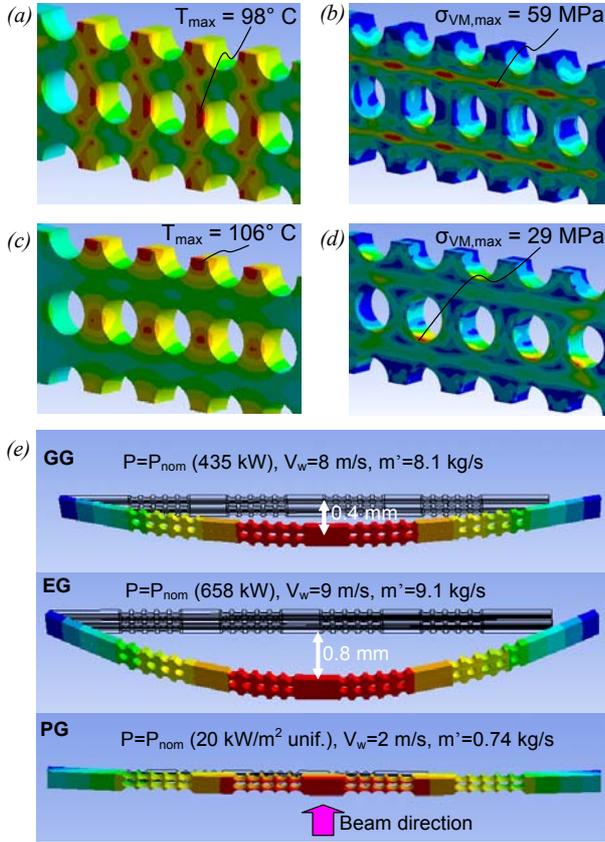

Fig. 5 - Thermo-structural analyses performed with the ANSYS code on the reference scenario: (a) and (b) Temperature and Von Mises equivalent stress on the EG; (c) and (d) Temperature and Von Mises equivalent stress on the GG; (e) Out of plane deformations of the three grids.

5. Compensation of Beamlet repulsion

As one of the techniques applied to compensate beamlet deflection due to the beamlet-beamlet interaction, aperture offset was examined numerically in a three grid accelerator at 500 kV in JT60U [21]. The trajectories of fifty beamlets from 10 x 5 apertures were traced utilizing the three dimensional beam analysis code, OPERA-3d. Fig. 6 shows the calculated beam footprints at 3.5 m downstream from the grounded grid. In Fig. 6a, the centers of all calculated beamlets are represented by points. They moved outward from the aperture positions due to the beamlet-beamlet interaction. The maximum deflection angle was 6 mrad in beamlet coming from peripheral apertures. The proper aperture offset to

compensate 6 mrad of beamlet deflection was evaluated to be 0.7 mm according to thin lens theory. Fig. 6b shows that all beamlets stay in positions extrapolated from the apertures by proper aperture offset at the bottom of extractor. The results have shown that a proper aperture offset within 1 mm is enough to correct the beamlet deflection by the beamlet-beamlet interaction. This compensation technique is to be applied to design 100 kV, 500 kV and 1 MeV accelerators.
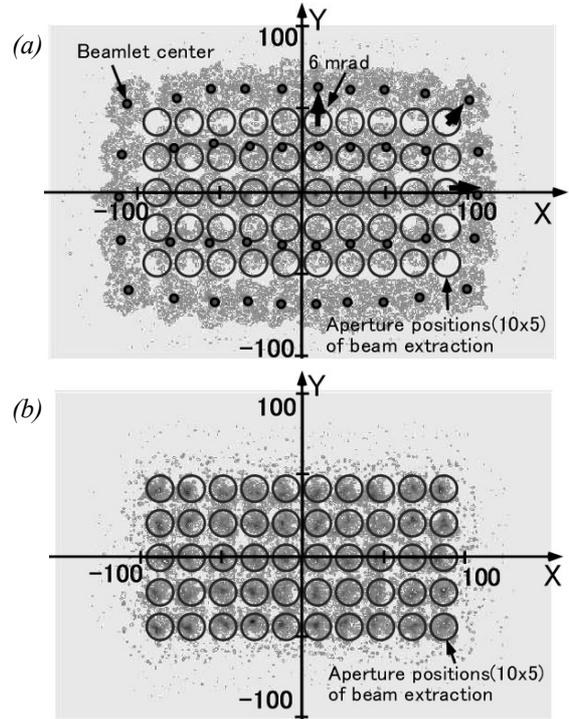

Fig. 6 - Calculated beam footprints at 3.5 m downstream from the grounded grid (a) before and (b) after proper aperture offset in the extractor. The beam parameter is 110 A /m^2 of D$^-$ ion beam current density and 340 keV at beam energy. Opened circles represent the original aperture positions.

6. Conclusions

The better understanding of the physics and the numerical tools available allow the optimisation of the accelerators for ITER to be carried out.

The procedure to optimize the 100 kV accelerator for ITER has been described with the present design of the accelerator. Using this procedure, the design of the extraction and acceleration system for the ITER NBI and related experiments can been accomplished by taking into account at the same time physics and engineering requirements.

References

[1] R. S. Hemsworth *et al*. Neutral beams for ITER. Rev. Sci. Instrum. 67, Issue 3, 1120 (1996).

[2] T. Inoue *et al*. Design of neutral beam system for ITER-FEAT, Fus. Eng. and Design 56-57 (2001) 517-521

[3] R.S. Hemsworth *et al*. Rev. Sci. Instrum. 79, 02C109 (2008).

[4] D. Marcuzzi *et al*. Detail design of the RF Source for the 1 MV Neutral Beam Test Facility. 25th Symposium on Fusion Technology,15-19 September 2008, Rostock, Germany.

[5] P. Sonato *et al*. The ITER full size plasma source device design. 25th Symposium on Fusion Technology,15-19 September 2008, Rostock, Germany.

[6] M. Taniguchi *et al*. Development of 1 MeV H- accelerator at JAEA for ITER NB, to be published in Conf. Proc. of American Inst. Phys. 2008.

[7] H.P.L De Esch *et al*. Results of the SINGAP neutral beam accelerator experiment at JAEA, to be published to Fusion Eng. Design.

[8] M. Kashiwagi *et al*. R&D progress of high power negative ion accelerator for ITER NB system at JAEA, to be published to Nuclear Fusion.

[9] H.P.L. de Esch, R.S. Hemsworth and P. Massmann. Updated physics design ITER-SINGAP accelerator. Fusion Eng. Des. 73 (2005) 329.

[10] ITER Technical Basis 2002. Neutral beam heating & current drive (NB H&CD) system, Detailed Design Document (section 5.3 DDD5.3) (Vienna: IAEA)

[11] J. Pamela. A model for negative ion extraction and comparison of negative ion optics calculations to experimental results. Rev. Sci. Inst. 62 (1991) 1163.

[12] W.B. Hermannsfeld. Electron Trajectory Program, SLAC report, Stanford Linear Accelerator Center, SLAC-226 (1979)

[13] M. Cavenago *et al*. IEEE Trans. Plasma Sci. 36, 1581 (2008)

[14] G. Fubiani *et al*. Modeling of secondary emission processes in the negative ion based electrostatic accelerator of the International Thermonuclear Experimental Reactor. Phys. Rev. Special Topics Accelerators and Beams 11, 014202 (2008)

[15] "OPERA-3d", Vector Fields Co.Ltd., http://www.vectorfields.com/

[16] P. Agostinetti *et al*. Design of a low voltage, high current extraction system for the ITER Ion Source. AIP Proceedings of the 1st International Conference on Negative Ions, Beams and Sources, 2008, Aix en Provence, France.

[17] P. Agostinetti, S. Dal Bello, M. Dalla Palma, D. Marcuzzi, P. Zaccaria, R. Nocentini, M. Fröschle, B. Heinemann and R. Riedl. Thermomechanical design of the ITER Neutral Beam Injector grids for Radio Frequency Ion Source and SINGAP Accelerator. 22nd IEEE/NPSS Symposium on Fusion Engineering, Albuquerque, New Mexico, 2007.

[18] E. Speth *et al*. Overview of the RF source development programme at IPP Garching. Nucl. Fusion 46 (2006) S220-S238.

[19] Various Authors. ITER SDC-IC, Structural Design Criteria for ITER In-Vessel Components. ITER Document No. G 74 MA 8.

[20] P. Agostinetti, S. Dal Bello, M. Dalla Palma and P. Zaccaria. Thermomechanical design of the SINGAP accelerator grids for ITER NB Injectors. Fusion Eng. Des. 82 (2007) 860-866.

[21] M. Kashiwagi *et al*. Compensation of beamlet repulsion in a large negative ion source with a multi aperture accelerator. AIP Proceedings of the 1st International Conference on Negative Ions, Beams and Sources, 2008, Aix en Provence, France.